# Index Modulated Spectral Efficient Frequency Division Multiplexing Assisted by Lower Order Modulations

Muhammad Sajid Sarwar
*Department of IT Convergence Engineering*
*WENS Laboratory, Kumoh National Institute of Technology*
Gumi, South Korea
sajid.sarwar@kumoh.ac.kr

Soo Young Shin Senior Member, IEEE
*Department of IT Convergence Engineering*
*WENS Laboratory, Kumoh National Institute of Technology*
Gumi, South Korea
wdragon@kumoh.ac.kr

***Abstract*—Spectral efficient frequency division multiplexing with index modulation (SEFDM-IM) transmits information through predefined subcarriers' activation patterns along with $M$-ary constellation symbols. It employs non-orthogonal subcarriers to enhance the spectral efficiency (SE) of classical orthogonal frequency division multiplexing with index modulation (OFDM-IM). SEFDM-IM improves the bit-error rate (BER) when compared to classical SEFDM at the same spectral efficiency (SE). The inactive subcarriers of SEFDM-IM aid in reducing inter-carrier interference; however, higher-order modulations to improve SE can erode this achievement and contribute to BER degradation. This paper suggests lower-order modulation-assisted SEFDM-IM (LSEFDM-IM) to achieve high SE by increasing index bits and sending fewer bits via the constellation symbols. For this purpose, certain index combinations of conventional SEFDM-IM are reused with the help of distinguishable lower-order constellations. LSEFDM-IM outperforms conventional SEFDM-IM and traditional lower-order modulation-aided OFDM-IM in terms of inter-symbol interference, BER, and SE.**

***Index Terms*—Index modulation (IM), ICI, ISI, lower-order modulations, OFDM, SEFDM, SEFDM-IM.**

## I. Introduction

Orthogonal frequency division multiplexing (OFDM) is a key technology in various wireless communication standards due to its robustness to frequency selective fading channels and inter-symbol-interference (ISI). In next-generation wireless networks, bandwidth has become a valuable resource because of high connectivity and the rapidly increasing demands for data rates. To meet these requirements, several schemes like index modulation (IM) were proposed that transmit $M$-ary constellation symbols over an active pattern of transmission entities such as antennas, subcarriers, or time slots to convey additional information via activation pattern in an energy-efficient manner [1], [2]. OFDM with IM (OFDM-IM) has employed partially activated subcarriers to carry $M$-ary symbols. The input bits were used to design this activation pattern which could also be decoded as information at the receiver [3], [4]. The virtual transmission of index bits provides an attractive trade-off among spectral efficiency (SE), bit-error-rate (BER), energy efficiency (EE), and transceiver complexity [1]. Also, in [4], it was suggested as a suitable technique for mobile users where the subchannel orthogonality of the traditional OFDM could lose due to rapid variation of the wireless channel leading to inter-carrier-interference (ICI). The inactive subcarriers of OFDM-IM reduce the impact of ICI but as far as SE is concerned, the conventional OFDM-IM cannot surpass standard OFDM due to partially activated subcarriers if the same constellation size is used for both schemes [5]. In terms of SE, OFDM-IM can outperform OFDM either by using higher-order modulations at the expense of increased error performance or by using all subcarriers with distinguishable constellation modes such as dual-mode OFDM (DM-OFDM) [6] and multi-mode OFDM (MM-OFDM) [7] with IM. Lower-order modulation-aided OFDM-IM (LOFDM-IM) was proposed in [8] which has increased index information by reusing the index combinations with the help of distinguishable lower-order modulations. The subcarriers were partially activated, making LOFDM-IM robust to ISI and improving EE compared to DM-OFDM and MM-OFDM. In addition, the index information was transmitted virtually and did not require extra energy for transmission, which also aided in the BER improvement of typical OFDM-IM [8].

SEFDM was proposed to improve the SE of classical OFDM by designing non-orthogonal subcarriers at the cost of enhanced ICI [9], [10]. It violated orthogonality to enhance data rate, or the same amount of data could be transmitted using less bandwidth compared to the OFDM system. It could double the connectivity of internet-of-things devices [11]. Non-orthogonal subcarriers were generated by reducing subcarrier spacing (SCS) $\Delta f$ of a typical OFDM system. SEFDM maintained signal duration $\tau$ while SCS $\Delta f < 1/\tau$ which could lead to BER degradation due to substantial uncontrolled intersymbol interference (ISI) on adjacent subcarriers, particularly at higher modulation orders [12]. Also, the violation of orthogonality makes the detection of received signals challenging due to overlapping subcarriers [10]. In SEFDM-IM, the self-created ICI was reduced by partially activating subcarriers, but higher-order constellations could worsen BER performance due to enhanced ISI [13]–[15].

In this proposed work, the authors aim to improve the BER

and SE of SEFDM-IM by proposing lower-order modulation-assisted SEFDM-IM (LSEFDM-IM). Instead of using a higher constellation size to enhance SE at the expense of BER, it increases the number of index bits by reusing certain index combinations of traditional SEFDM-IM with the aid of distinguishable lower-order constellation modes. This study differs from the MM-OFDM approach, which employs differentiable constellation alphabets to use all subcarriers. Like SEFDM-IM, it has inactive subcarriers that enlarge the Euclidean distance between the modulated symbols and help to lower the ICI and ISI of the classical SEFDM system. As SEFDM can accommodate more subcarriers in a given bandwidth compared to an OFDM system, the detection complexity of the typical maximum likelihood detector rises exponentially. Therefore, the article suggests low-complexity decoders such as minimum mean-square error (MMSE) and log-likelihood ratio (LLR) detectors for LSEFDM-IM whose complexity does not grow exponentially with the number of subcarriers. The proposed scheme outperforms conventional OFDM, SEFDM, OFDM-IM, SEFDM-IM, and LOFDM-IM in terms of SE, ISI, and BER. Additionally, the analytical and simulation outcomes corroborate the advantages of the LSEFDM-IM.

## II. System Model

The illustration of the transmitter block is provided in Fig. 1. The LSEFDM-IM system is built on a SEFDM system containing $N_F$ subcarriers. At the transmitter, $B$ bits are divided into $G$ groups such that each group contains $b$ bits. In each group, $b$ bits are divided into $b_1$ index bits and $b_2$ constellation bits. Each group equally participates in the formation of LSEFDM-IM subblocks. There are $G$ subblocks having $N = N_F/G$ subcarriers in each. The first $b_1 = \left\lfloor \log_2 \left( \begin{array}{c} N \\ K \end{array} \right) \right\rfloor$ bits are used to select a combination of $K$ active subcarriers out of $N$ in each sub-block, while the rest of $N-K$ subcarriers are set to zero. A simplified example of an index pattern is provided through a look-up table (LUT) in Table I. It is known both at the transmitter and the receiver. A lower-order modulation $M^{'} < M$ is adopted to transmit $b_2 = \log_2 M^{'}$ bits over $K$ subcarriers, where $M$ and $M^{'}$ refer to the modulation order used for conventional SEFDM-IM and the proposed LSEFDM-IM, respectively. Unlike conventional SEFDM-IM, an active combination of subcarriers is reused with the aid of $m$ distinguishable modes indicated as $M_q^{'}$ where $q = 1, 2, \cdots, m$. For example, $[1, 0, 0, 0]$ pattern is chosen by $000$ or $100$ in Table I. In a conventional IM scheme, the receiver does not have any knowledge to decode $000$ or $100$ for that particular active pattern. In the suggested scheme, if the receiver detects $M_1$ for $[1, 0, 0, 0]$, it decodes $000$ additionally as $b_1$. On the other hand, if it gets $M_2$ for $[1, 0, 0, 0]$, it will decode $100$. It is important to mention that the different alphabets used in Table I are readily differentiable because $M_1^{'} \cap M_2^{'} \cap \cdots \cap M_m^{'} = \phi$. The reuse of index combinations helps carry more information as index bits. Moreover, in some cases, like $K = 2$ and $N = 4$, there are six possible combinations, but only four of them can be used in traditional SEFDM-IM; the other two are discarded, but they can be used in the proposed method. The transmitted bits in SEFDM-IM and LSEFDM-IM by a group $g \in G$ are compared in (1) and (2)

$$b = b_1 + b_2 = \left\lfloor \log_2 \left( \begin{array}{c} N \\ K \end{array} \right) \right\rfloor + K \log_2 M, \tag{1}$$

$$\begin{aligned} b &= b_1^{'} + b_2^{'} = (b_1 + p) + b_2^{'}, \\ &= \left\lfloor \log_2 \left( \begin{array}{c} N \\ K \end{array} \right) \right\rfloor + p + K \log_2 M_q^{'}, \end{aligned} \tag{2}$$

where $p = K \log_2 M - K \log_2 M_q^{'}$ provides extra index information that does not require energy for transmission but is virtually embedded to compensate the loss due to $K \log_2 M_q^{'} < K \log_2 M$. Therefore, in the newly adopted scheme $b_1^{'} > b_1$ and $b_2^{'} < b_2$ which makes LSEFDM-IM more energy efficient and robust to ISI and ICI compared to SEFDM-IM.

For the $g_{th}$ group, the active indices based on $b_1^{'}$ are

$$\mathbf{i}^g = \left[ i^g(1)\, i^g(2) \cdots i^g(K) \right]^{\mathrm{T}}, \tag{3}$$

where $i^g(k)$ is an active index from $k = 1, 2, \cdots, K$ and $K \subset N$. These active subcarriers can carry modulated data $\mathbf{s}_g$ over $\mathbf{i}_g$ based on the predefined rule in Table I.

$$\mathbf{s}^g = \left[ s^g(1)\, s^g(2) \cdots s^g(K) \right]^{\mathrm{T}}, \tag{4}$$

where $s^g(k)$ represents a symbol of a constellation alphabet. It is assumed that symbols are normalized to have unit average power, i.e., $E\{\mathbf{s}^g \left(\mathbf{s}^g\right)^H\} = K$. As $s^g(k)$ belongs to a distinct alphabet depending on index information, it is described as

$$s^g(k) = \mathcal{S}_q(k) \in M_q^{'}, \quad q = 1, 2, \cdots, m, \tag{5}$$

here each $M_q^{'}$ has the same size, e.g., $|M_1^{'}| = |M_2^{'}| \cdots = |M_m^{'}|$ but is rotated at an angle such that these are distinguishable at the receiver. The average symbol power and the minimum Euclidean distance (MED) do not change with the rotation of a constellation for a finite value of $M^{'}$. For constellation rotation, a principle similar to [7] is adopted, which is briefed here. If an ordinary $M^{'}$-PSK is considered, its points are located on a unit circle having MED $d_{med}^{\mathrm{PSK}}(M^{'}) = 2 \sin\left(\frac{\pi}{M^{'}}\right)$. In the proposed scheme, differentiable modes are required, which can be generated by rotating the basic $M^{'}$-PSK at an angle of $2\pi j(q-1)/(M^{'}m)$ where $q = 1, 2, \cdots, m$. These $m$ modes are distributed uniformly in a circle to maximize the minimum inter-mode distance (MIRD). In the adopted method, MIRD becomes MED of an $M^{'}m$-PSK constellation, and it is given as

$$d_{mird}^{\mathrm{PSK}}(M^{'}, m) = d_{med}^{\mathrm{PSK}}(M^{'}m) = 2 \sin\left(\frac{\pi}{M^{'}m}\right). \tag{6}$$

In other words, if four sets of BPSK are designed by this rotation rule, jointly these will be equal to 8-PSK, with all points distributed uniformly in a circle. Therefore, these modes are readily distinguishable at the receiver. The number of rotated versions of the constellation is calculated as

$$m = \left\lceil 2^{(b_1+p)} / \left( \begin{array}{c} N \\ K \end{array} \right) \right\rceil, \tag{7}$$

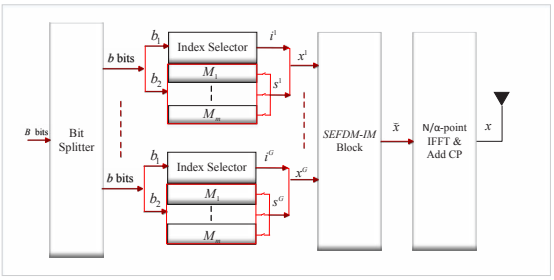


Fig. 1. Transmitter block diagram for LSEFDM-IM.

where $\lceil \cdot \rceil$ represents the ceiling function. After generating $G$ sub-blocks according to the procedure discussed so far, these are concatenated to form a block as follows

$$\breve{\mathbf{x}} = [\breve{x}(1)\ \breve{x}(2) \cdots \breve{x}\,(N_F)]^{\mathrm{T}} \quad = \left[ \left(\mathbf{x}^1\right)^{\mathrm{T}} \left(\mathbf{x}^2\right)^{\mathrm{T}} \cdots \left(\mathbf{x}^G\right)^{\mathrm{T}} \right]^{\mathrm{T}}, \tag{8}$$

where $\mathbf{x}^g$ indicates a symbol vector $\mathbf{s}^g$ riding over $\mathbf{i}^g$ and $g \in \{1, 2, \cdots, G\}$. For $G$ sub-blocks, (8) can be expanded as $\breve{\mathbf{x}} = \left[x^1(1), \cdots x^1(N),\ x^2(1), \cdots x^2(N),\ \cdots x^G(1), \cdots x^G(N)\right]^{\mathrm{T}}$. The subcarriers of LSEFDM-IM are allocated in a non-orthogonal manner to increase SE. SCS is compressed such that the frequency domain separation among these is less than in a typical OFDM system. The bandwidth compression factor is given as $\alpha = \Delta f \tau$ where $\Delta f$ and $\tau$ denote minimum frequency domain subcarrier spacing and time domain symbol period, respectively, and $0 < \alpha < 1$. If $\alpha = 1$, it indicates the classical case of orthogonal subcarriers. The transmission rate R in [bps/Hz] for any group of LSEFDM-IM is formulated from (2) as $\mathrm{R} = \frac{b}{\alpha N}$. It demonstrates that R increases as the $\alpha$ declines, e.g., subcarrier spacing is compressed more and more. To generate non-orthogonal subcarriers, there are mainly two methods in the literature (i). single inverse fast Fourier transform (IFFT), (ii). multiple IFFT [16]. Following a single IFFT, the time-domain signal is given as

$$\mathbf{x} = \frac{1}{\sqrt{\tau}} \sum_{n=0}^{N_F - 1} \breve{\mathbf{x}} \exp(j2\pi n \alpha \mathrm{t}/\tau). \tag{9}$$

The time domain symbols derived from the IFFT process are normalized to have the unit energy $E\left\{\mathbf{x}^{\mathrm{H}}\mathbf{x}\right\} = N_F$. The cyclic prefix ($C_P$) is inserted to reduce ISI. The $C_P$ is longer than the maximum delay spread of the channel; therefore, $C_P > L$ where $L$ stands for channel tap length. The signal is now transmitted over a frequency-selective Rayleigh fading channel. The received signal is written as

$$\mathbf{y} = \mathrm{diag}\,(\mathbf{x})\,\mathbf{h} + \mathbf{z}. \tag{10}$$

The received signal vector $\mathbf{y}$ is expanded as $\mathbf{y} = \begin{bmatrix} y(1) & y(2) & \cdots & y\,(N_F) \end{bmatrix}^{\mathrm{T}}$. The channel between the transmitter and the receiver is given by $\mathbf{h} \in \mathbb{C}^{N_F \times 1}$ which is assumed to follow the $\mathcal{CN}(0,1)$ distribution. The noise vector is indicated by $\mathbf{z} \in \mathbb{C}^{N_F \times 1}$ which follows the $\mathcal{CN}\,(0, N_{0,F})$ complex Gaussian distribution with $N_{0,F}$ as the variance of the frequency domain noise. Its time-domain counterpart is expressed as $N_{0,F} = (\frac{K}{N}) N_{0,T}$. The signal-to-noise ratio is given by $\frac{E_b}{N_{0,T}}$ where $E_b = \frac{N_F + C_P}{B}$ is the average transmitted energy per bit. The SE of LSEFDM-IM is calculated as $\frac{B}{\alpha(N_F + C_P)}$ bits/s/Hz.

TABLE I
AN EXAMPLE OF LUT

| Index Bits | Index combination | Modulation |
|---|---|---|
| 000 | [1,0,0,0] | $M_1^{'}$ |
| 001 | [0,2,0,0] | |
| 010 | [0,0,3,0] | |
| 011 | [0,0,0,4] | |
| 100 | [1,0,0,0] | $M_2^{'} = PSK\left(M_1^{'}\right) \times exp\left(\frac{2\pi j(q-1)}{m M_1^{'}}\right)$ where $q = 1, \cdots, m$ |
| 101 | [0,2,0,0] | |
| 110 | [0,0,3,0] | |
| 111 | [0,0,0,4] | |

### A. Detection

The received signal is separated into $g$ groups before detection, and $\mathbf{y}^g$ as the signal of $g_{th}$ group is written below.

$$\mathbf{y}^g = \mathrm{diag}\,(\mathbf{x}^g)\,\mathbf{h}^g + \mathbf{z}^g. \tag{11}$$

For the $g_{th}$ group, the transmitted vector $\mathbf{x}^g$, the received signal $\mathbf{y}^g$, the noise vector $\mathbf{z}^g$ and the corresponding channel are given in (12), (13), (14) and (15), respectively.

$$\mathbf{x}^g = [x^g(1)\, x^g(2) \cdots x^g(N)]^{\mathrm{T}}. \tag{12}$$

$$\mathbf{y}^g = [y^g(1)\, y^g(2) \cdots y^g(N)]^{\mathrm{T}}. \tag{13}$$

$$\mathbf{z}^g = [z^g(1)\, z^g(2)\ \cdots\ z^g(N)]^{\mathrm{T}}. \tag{14}$$

$$\mathbf{h}^g = [h^g(1)\, h^g(2)\ \cdots\ h^g(N)]^{\mathrm{T}}. \tag{15}$$

#### 1) ML Detection

A joint detection is considered in $g$ groups assuming channel state information (CSI) is known at the receiver. For single-tap equalization, CSI is acquired before data transmission by sending OFDM pilots at a lower rate than SEFDM. The optimal ML detection is expressed as

$$\left(\hat{\mathbf{x}}^g, \hat{\mathbf{i}}^g\right)_{\mathrm{ML}} = \arg \min_{\left(\hat{\mathbf{x}}^g, \hat{\mathbf{i}}^g\right)} \left\| \mathbf{y}^g - \mathrm{diag}\,(\mathbf{x}^g)\,\mathbf{h}^g \right\|^2, \tag{16}$$

where $\| \cdot \|$ represents the Euclidean norm. The ML achieves optimal performance at the cost of complexity, which grows exponentially with a linear increase in subcarriers. The search complexity per sub-block is of the order of $M^{'K} \binom{N}{K} m$ where $m$ is provided in (7). Therefore, it is suitable for a limited number of subcarriers.

#### 2) MMSE-ML Detection

To reduce the complexity of the ML decoder, successive detection is performed using linear MMSE followed by ML [13]. The received symbols are estimated using MMSE as given below

$$\hat{\mathbf{s}}_{\mathrm{mm}}^{(g)} = \frac{\{\mathbf{h}^g\}^H}{N/K} \left( \frac{\mathbf{h}^g \{\mathbf{h}^g\}^H}{N/K} + N_{0,F} \mathbf{I} \right)^{-1} \mathbf{y}^g, \tag{17}$$

where $\hat{\mathbf{s}}_{\mathrm{mm}}^{(g)}$ denotes MMSE-filtered symbols, e.g., $\hat{\mathbf{s}}_{\mathrm{mm}} = \left[\hat{\mathbf{s}}_{\mathrm{mm}}^{(1)}, \ldots, \hat{\mathbf{s}}_{\mathrm{mm}}^{(g)}\right]^T$. The notations $\mathbf{I}$ and $N_{0,F}$ indicate the identity matrix and the variance of the received noise, respectively.

Afterward, modulated bits of the $g_{th}$ sub-block are decoded by an exhaustive ML search as expressed below

$$\hat{\mathbf{b}}^{(g)}_{\mathrm{mmse-ml}} = \arg\min_{\mathbf{b}^{(g)}} \left\{ \left\| \hat{\mathbf{s}}^{(g)}_{\mathrm{mm}} - \mathbf{s}^{(g)} \right\|^2 \right\}. \tag{18}$$

The complexity of the MMSE-ML detection for the whole system containing $N_F$ subcarriers is of the order of $\binom{N}{K} m(N_F)^3$ where $b$ is defined in (2). It can be seen that the complexity of this detector does not grow exponentially with the increase in the number of subcarriers, as opposed to ML described in sub-section II-A1. The proposed scheme employs sub-block by sub-block detection, whereas contrary to (18) the conventional SEFDM system uses symbol-by-symbol detection, as mentioned in [17].

*3) MMSE-LLR*

Successive detection by MMSE and exhaustive ML search exhibit high complexity due to the large search space of (18). To reduce associated complexity, LLR detection is enabled by employing the signal filtered through MMSE [13]. As the detection procedure is identical in all groups, the process for the $g^{th}$ group is described only, and the superscript $g$ is omitted for brevity.

$$\gamma_q(n) = \ln\left( \frac{\sum_{j=1}^{M'} \Pr\left(s(n) = \mathcal{S}_q^j \mid \hat{s}_{\mathrm{mm}}(n)\right)}{\Pr\left(s(n) = 0 \mid \hat{s}_{\mathrm{mm}}(n)\right)} \right). \tag{19}$$

The higher value of $\gamma_q(n)$ refers to the high probability of $n^{th}$ subcarrier being modulated by a symbol from $q^{th}$ constellation mode. $\mathcal{S}_q^j$ is the $j^{th}$ symbol of $M_q^{'}$-PSK constellation. Now, by considering $\sum_{j=1}^{M'} \Pr\left(x(n) = \mathcal{S}_q^j\right) = \frac{K}{N}$ and $\Pr\left(x(n) = 0\right) = \frac{N-K}{N}$ as prior probabilities, the following expression can be written with the Bayes rule,

$$\begin{aligned} \gamma_q(n) = \ln(K) + \ln(N-K) + \frac{|s(n)|^2}{N_{0,F}} + \\ \ln\left( \sum_{j=1}^{M'} \exp\left( -\frac{\left|s(n) - \mathcal{S}_q^j(n)\right|^2}{N_{0,F}} \right) \right). \end{aligned} \tag{20}$$

The direct calculation of LLR values from $\mathbf{y}$ could impose considerable complexity for the larger size of $N_F$. Therefore, to avoid numerical overflow, the Jacobian logarithm similar to [6] is used to calculate $\ln\left( \sum_{j=1}^{M'} \exp\left( -\frac{\left|s(n) - \mathcal{S}_q^j(n)\right|^2}{N_{0,F}} \right) \right)$. The active subcarriers modulated with a particular mode are identified as follows:

$$\hat{i}(n) = max[\gamma_1(n),\, \gamma_2(n), \cdots, \gamma_q(n)]. \tag{21}$$

After determining the activation pattern, the corresponding symbols of a particular mode are estimated based on a single subcarrier-based ML search. The complexity of this decoder is $\mathcal{O}(N)$ which grows linearly with the number of subcarriers.

## III. Performance Evaluation

### A. Bit-Error-Rate Bound

This section provides the analytical BER bound for the proposed LSEFDM-IM scheme. The pairwise error events inside various sub-blocks are similar; therefore, investigating the error probability for a single sub-block is sufficient to evaluate the overall error performance of the suggested system. Assuming $\mathbf{x}^g$ is the modulated symbol, which is incorrectly demodulated as $\hat{\mathbf{x}}^g$ at the receiver, the conditional pairwise error probability (PEP) using ML detection is calculated as

$$\Pr(\mathbf{x}^g \to \hat{\mathbf{x}}^g | \mathbf{h}^g) \le Q\left( \sqrt{\frac{\|(\mathbf{x}^g - \hat{\mathbf{x}}^g)\mathbf{h}^g\|_F^2}{2N_{0,F}}} \right), \tag{22}$$

where $Q(x)$ is the Q-function, which can be approximated as $Q(x) \cong \frac{1}{12}e^{-x^2/2} + \frac{1}{4}e^{-2x^2/3}$, similar to [18]. The unconditional PEP (UPEP) is formulated by averaging (22) using the approximate form of $Q(x)$. It is expressed as follows:

$$\begin{aligned} P(\mathbf{x}^g \to \hat{\mathbf{x}}^g) \cong E\left\{ \frac{1}{12} \exp\left( -\frac{\|(\mathbf{x}^g - \hat{\mathbf{x}}^g)\mathbf{h}^g\|_F^2}{4N_{0,F}} \right) \right. \\ \left. + \frac{1}{4} \exp\left( -\frac{\|(\mathbf{x}^g - \hat{\mathbf{x}}^g)\mathbf{h}^g\|_F^2}{3N_{0,F}} \right), \right. \end{aligned} \tag{23}$$

Now, average bit-error-probability is evaluated using UPEP

$$P_b \le \frac{1}{b2^b M'^K} \sum_{\mathbf{x}^g} \sum_{\hat{\mathbf{x}}^g} d(\mathbf{x}^g, \hat{\mathbf{x}}^g) P(\mathbf{x}^g \to \hat{\mathbf{x}}^g), \tag{24}$$

where $b$ is expressed in (2). The possible realizations of $\mathbf{x}^g$ are given by $2^b M'^K$. Moreover, $d(\mathbf{x}^g, \hat{\mathbf{x}}^g)$ denotes the Hamming distance between transmitted and the estimated signal corresponding to $P(\mathbf{x}^g \to \hat{\mathbf{x}}^g)$.

## IV. Result Discussion

This section presents the performance of the proposed LSEFDM-IM in terms of SE, ISI, and BER and compares them with benchmarks such as classical OFDM, SEFDM, OFDM-IM, LOFDM-IM, and SEFDM-IM. For result analysis, it is assumed that CSI is completely known at the receiver and that the transmitter and receiver are perfectly synced. Additionally, the pertinent simulation parameters are provided in the explanation of each illustration.

Fig. 2 (a) shows that if the same number of bits are transmitted using typical SEFDM-IM and proposed LSEFDM-IM, the latter can transmit more bits via index information than the former. For this illustration, $M = 4$, $M^{'} = 2$, $N = 8$ and $K = 1, 2, \cdots, 7$ are used. The suggested technique transmits 10 index bits at $b = 14$ and maintains them until $b = 17$, whereas SEFDM-IM transmits a maximum of 6 bits as index information at $b = 14$ (refer to (1) and (2)). Also, in SEFDM-IM, index information starts decreasing when more than $N/2$ subcarriers are active. In Fig. 2 (b), it is shown that the proposed scheme can achieve an SE similar to SEFDM-IM at $M^{'} = M/2$. It will aid in reducing ISI induced by non-orthogonal subcarriers. The modulation size corresponding to each curve is provided in the legend of Fig. 2 (b).

Fig. 2 (c) depicts the ISI comparison among LSEFDM-IM and its conventional counterparts. It can be seen that SEFDM has the highest ISI due to the violation of the orthogonality of standard OFDM. SEFDM-IM helps to reduce ISI because the partial activation enhances the Euclidean distance among the symbols. In LSEFDM-IM, ISI is even lower than in SEFDM-IM because the same SE can be achieved by enhancing index information and reducing the modulation size. It is

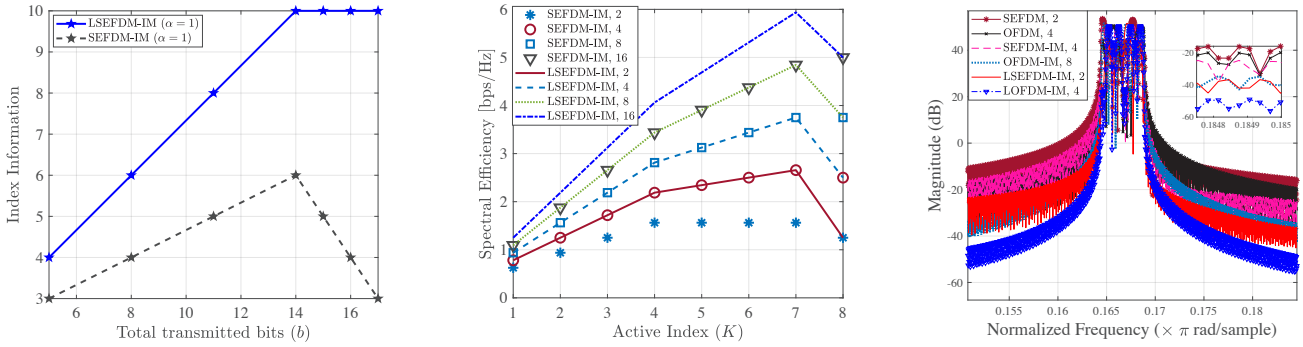


**(a)** **(b)** **(c)**

Fig. 2. **(a)** Index information vs total transmitted bits ($\alpha = 1$). & **(b)** SE w.r.t $K$ at $\alpha = 0.8$. **(c)** ISI comparison at $\alpha = 0.8$ for non-orthogonal subcarriers.

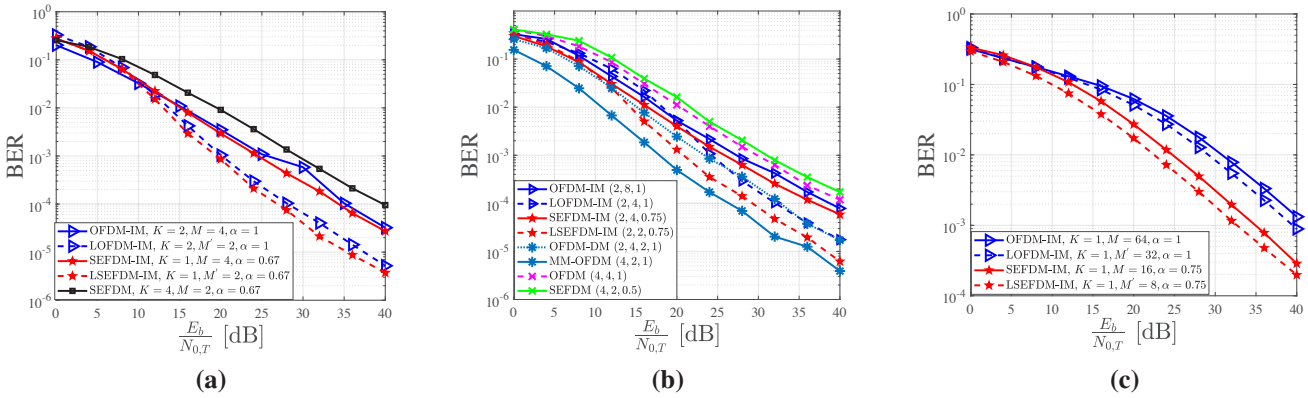


**(a)** **(b)** **(c)**

Fig. 3. **(a)** BER comparison of various schemes transmitting 6 bits. **(b)** BER comparison of different schemes transmitting 8 bits. **(c)** BER comparison of various schemes transmitting 8 bits.

higher compared to LOFDM-IM because of non-orthogonality. OFDM and LOFDM-IM are considered benchmarks for the sake of comparison. LOFDM-IM provides the lowest ISI as it can maintain orthogonality among the subcarriers. To perform simulation at the same SE, different modulation sizes are mentioned in the legend. Moreover, SEFDM uses $(\alpha = 0.5)$, while SEFDM-IM and LSEFDM-IM employ $(\alpha = 0.75)$.

Fig. 3 (a) illustrates the BER performance comparison to transmit 6 bits with LSEFDM-IM, LOFDM-IM, SEFDM-IM, and, OFDM-IM. The simulation parameters include $N_F = 512$, $N = 4$, and $G = 128$ while $K$, $M$, $M^{'}$, and $\alpha$ are mentioned in the legend corresponding to each curve. LSEFDM-IM outperforms all other schemes in this case because it uses the smallest constellation size with only one active subcarrier in each group. Lower activation and constellation reduce ICI and ISI, respectively, which improves the BER of the proposed system. The performance is compared with classical SEFDM, represented by $K = 4$ (non-IM case). In general, the lower order modulation-aided IM (LIM) systems have a high BER compared to the IM cases at low $E_b/N_{0,T}$ values, and as the $E_b/N_{0,T}$ increases, the BER of the LIM systems surpasses that of the IM variants. Compared to SEFDM-IM, the proposed technique achieves a nearly 8 dB gain to get a BER value of around $2{\times}10^{-05}$. Approximately 3 dB of gain can be observed in LSEFDM-IM as compared to LOFDM-IM.

Fig. 3 (b) shows BER performance to transmit 8 bits using $N_F = 512$, $N = 4$, while other parameters are provided in the legends which follow these notations; $(K, M, \alpha)$ and $(K, M^{'}, \alpha)$, $(K, M_a, M_b, \alpha)$, and $(N, M_j, \alpha)$, for OFDM-IM/SEFDM-IM and LOFDM-IM/LSEFDM-IM, OFDM-DM, and MM-OFDM, respectively. Here, OFDM, SEFDM, OFDM-DM, and MM-OFDM are used as benchmark techniques. A trend similar to Fig. 3 (a) is observed in LIM and IM schemes. LSEFDM-IM performs better than OFDM-DM as well because the predecessor requires a modulation size of 2 with only 2 subcarriers active in each group, while the successor needs constellation A, $M_a = 4$ over 2 selected subcarriers, and constellation B, $M_b = 2$ over the remaining two subcarriers in each group. It should be noted that in both cases, constellations are distinguishable, and lower constellations, along with partial activation of subcarriers aids LSEFDM-IM in outperforming OFDM-DM. On the other hand, the BER of the proposed system lags 2 to 3 dB behind MM-OFDM as the same constellation size is used in both scenarios to achieve the same SE. Despite the fact that LSEFDM-IM employs partial activation, MM-OFDM's BER is slightly better due to its orthogonal subcarriers.

Fig. 3 (c) compares the BER of OFDM-IM and LOFDM-

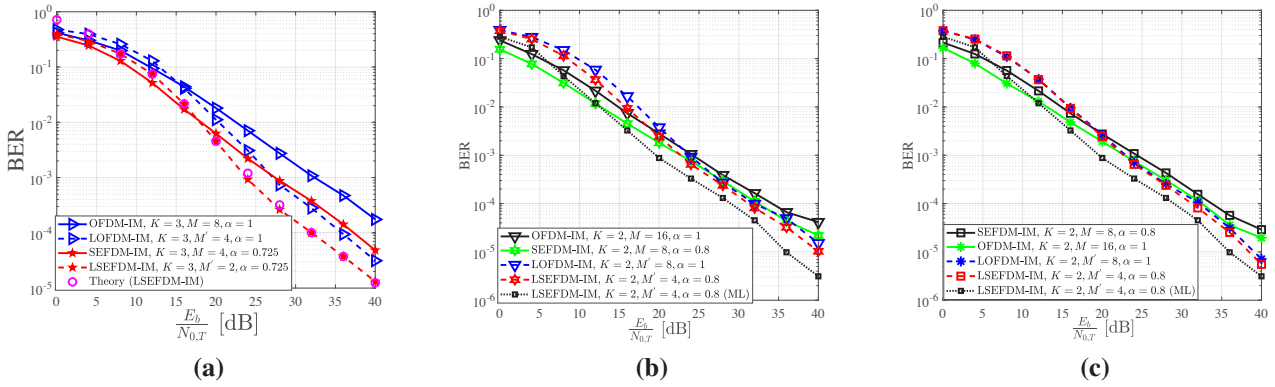


Fig. 4. **(a)** BER comparison of different schemes transmitting 11 bits. **(b)** BER performance with MMSE. **(c)** BER performance with MMSE-LLR.

IM employing $M = 64$ and 32, respectively, to transmit 8 bits using $N_F = 64$, $G = 16$, $N = 4$, and $K = 1$. SEFDM-IM and LSEFDM-IM outperform their orthogonal counterparts because the same number of bits are delivered with $M = 16$ and 8, respectively. In Fig. 4 (a), the BER of four different schemes is compared to transmit 11 bits in each case by using $N_F = 512$, $N = 4$. LSEFDM-IM attains almost 10, 5, and 4 dB gain to achieve a BER of around $1 \times 10^{-04}$ as compared to OFDM-IM, SEFDM-IM, and LOFDM-IM, respectively. Also, the theoretical error bound of the proposed technique is consistent with the computer simulation.

The BER performance using the MMSE-ML and MMSE-LLR decoders is shown in Fig. 4 (b) and (c), respectively. When compared to the best case of ML, MMSE-LLR offers lower complexity than MMSE-ML at a cost of nearly 2 dB and 3 dB BER performance loss, respectively.

## V. Conclusion

LSEFDM-IM was proposed to achieve SE similar to conventional SEFDM-IM with lower-order modulations. The enhanced index information did not require extra energy for transmission and supported achieving the desired SE at the expense of enhanced complexity. Lower-order constellations helped to reduce ISI induced by non-orthogonal subcarriers. The performance of LSEFDM-IM has been compared with traditional benchmarks such as OFDM, SEFDM, OFDM-IM, LOFDM-IM, and SEFDM-IM. It reveals that the suggested scheme outperformed its counterparts in terms of SE and BER. The investigation of LSEFDM-IM for mobile terminals with rapidly changing wireless channels would be interesting.

## VI. Acknowledgment

This research was supported by the MSIT (Ministry of Science and ICT), Korea, under the ICAN (ICT Challenge and Advanced Network of HRD) program (IITP-2022-RS-2022-00156394) supervised by the IITP (Institute of Information Communications Technology Planning Evaluation).

## References

[1] S. Doğan Tusha, A. Tusha, E. Basar, and H. Arslan, "Multidimensional index modulation for 5G and beyond wireless networks," *Proc. IEEE*, vol. 109, no. 2, pp. 170–199, 2021.

[2] M. Alzard, S. Althunibat, K. Umebayashi, and N. Zorba, "Resource allocation in THz-based subcarrier index modulation systems for mobile users," in *IEEE GLOBECOM*, 2021.

[3] D. Tsonev, S. Sinanovic, and H. Haas, "Enhanced subcarrier index modulation (SIM) OFDM," in *Proc. GLOBECOM Workshops*, 2011, pp. 728–732.

[4] E. Basar, U. Aygolu, E. Panayirci, and H. V. Poor, "Orthogonal frequency division multiplexing with index modulation," *IEEE Trans. Signal Process.*, vol. 61, no. 22, pp. 5536–5549, 2013.

[5] M. Wen, X. Cheng, M. Ma, B. Jiao, and H. V. Poor, "On the achievable rate of OFDM with index modulation," *IEEE Trans. Signal Process.*, vol. 64, no. 8, pp. 1919–1932, 2016.

[6] T. Mao, Z. Wang, Q. Wang, S. Chen, and L. Hanzo, "Dual-mode index modulation aided OFDM," *IEEE Access*, vol. 5, pp. 50–60, 2016.

[7] M. Wen, E. Basar, Q. Li, B. Zheng, and M. Zhang, "Multiple-mode orthogonal frequency division multiplexing with index modulation," *IEEE Trans. Commun*, vol. 65, no. 9, pp. 3892–3906, 2017.

[8] S. A. Nambi and K. Giridhar, "Lower order modulation aided BER reduction in OFDM with index modulation," *IEEE Commun. Lett.*, vol. 22, no. 8, pp. 1596–1599, 2018.

[9] I. Darwazeh, H. Ghannam, and T. Xu, "The first 15 years of SEFDM: A brief survey," in *in Proc. 11th Int. Symp. CSNDSP, Jul.*, 2018, pp. 1–7.

[10] T. Xu, C. Masouros, and I. Darwazeh, "Waveform and space precoding for next generation downlink narrowband IoT," *IEEE Internet Things J.*, vol. 6, no. 3, pp. 5097–5107, 2019.

[11] T. Xu and I. Darwazeh, "Non-orthogonal narrowband internet of things: A design for saving bandwidth and doubling the number of connected devices," *EEE Internet Things*, vol. 5, no. 3, pp. 2120–2129, 2018.

[12] M. Rodrigues and I. Darwazeh, "Fast OFDM: A proposal for doubling the data rate of OFDM schemes," in *Proc. Int. Conf. Telecommun.*, vol. 3, 2002, pp. 484–487.

[13] M. Nakao and S. Sugiura, "Spectrally efficient frequency division multiplexing with index-modulated non-orthogonal subcarriers," *IEEE Wireless Commun. Lett.*, vol. 8, no. 1, pp. 233–236, 2018.

[14] Y. Chen, T. Xu, and I. Darwazeh, "Index modulation pattern design for non-orthogonal multicarrier signal waveforms," *IEEE Trans. Wireless Commun.*, vol. 21, no. 10, pp. 8507–8521, 2022.

[15] M. S. Sarwar, M. Ahmad, and S. Y. Shin, "Subcarrier index modulation for spectral efficient frequency division multiplexing in multi-input multi-output channels," *IEEE Trans. Veh. Technol.*, vol. 72, no. 2, pp. 2678–2683, 2023.

[16] T. Xu and I. Darwazeh, "Transmission experiment of bandwidth compressed carrier aggregation in a realistic fading channel," *IEEE Trans. Veh. Technol.*, vol. 66, no. 5, pp. 4087–4097, 2017.

[17] I. Kanaras, A. Chorti, M. Rodrigues, and I. Darwazeh, "A combined MMSE-ML detection for a spectrally efficient non-orthogonal FDM signal," in *Proc. 5th Int. Conf. Broadband Commun. Netw. Syst.*, 2008, pp. 421–425.

[18] M. Chiani and D. Dardari, "Improved exponential bounds and approximation for the Q-function with application to average error probability computation," in *Proc. IEEE Global Telecommun. Conf, GLOBECOM '02.*, vol. 2, 2002, pp. 1399–1402 vol.2.